

Supporting Information

For

Michael addition-cyclization-based *switch-on* fluorescent chemodosimeter for Cysteine and its application in living cell imaging

Srimanta Manna,^a Parthasarathi Karmakar,^a Syed Samim Ali,^a Uday Narayan Guria,^a Ripon Sarkar,^b Pallab Datta,^b Debasish Mandal,^c Ajit Kumar Mahapatra^{*a}

^a Department of Chemistry, Indian Institute of Engineering Science and Technology, Shibpur, Howrah – 711103, India.

^b Centre for Healthcare Science and Technology, Indian Institute of Engineering Science and Technology, Shibpur, India

^c School of Chemistry and Biochemistry, Thapar Institute of Engineering and Technology, Patiala 147 004 Punjab, 486 India.

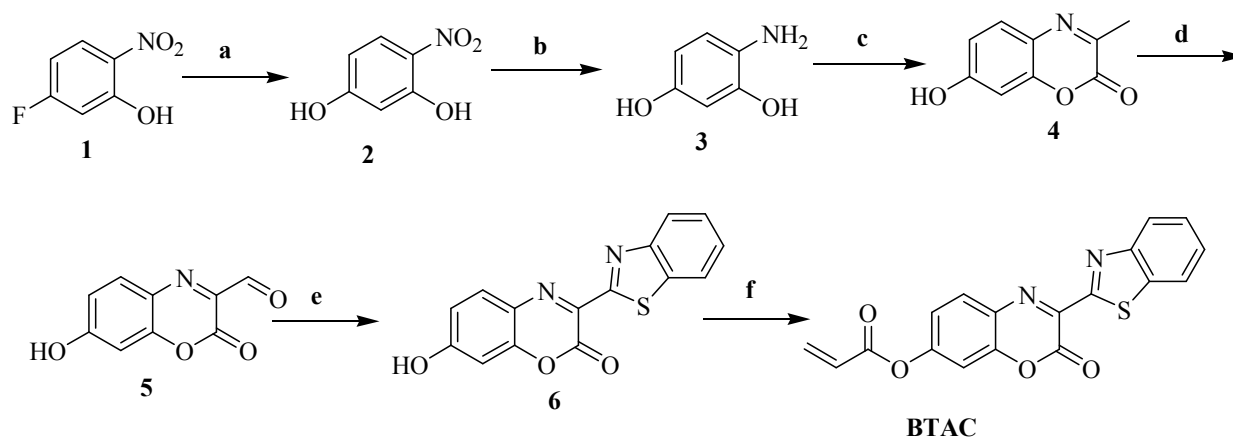
*Corresponding author. Fax: +91 33 26684564; Tel: +91 33 2668 4561;

E-mail: mahapatra574@gmail.com (A. K. Mahapatra)

Table of Contents

Description	page
1. Synthesis and characterization	2
2. Analytical data of compounds and intermediates	2- 7
3. Calculation for detection limit	8
4. Competitive Experiments of BTAC	8-9
5. Kinetic studies	10-11
6. Cytotoxic effect	11-12
7. Computational studies	12-13

Synthesis and characterization



Reagent & condition: (a) Aq. KOH, water, 90 °C, 12h, 60%; (b) 10% Pd-C, H₂ balloon, rt, 5h, crude; (c) Ethyl pyruvate, ethanol, reflux, 5h, 29%; (d) SeO₂, dioxane, 75 °C, 5h, 62%; (e) 2-Aminothiophenol, KHSO₄, reflux, 12h, 57% (f) Acryloyl chloride, Et₃N, DCM, 2h, 54%.

Analytical data of compounds and intermediates

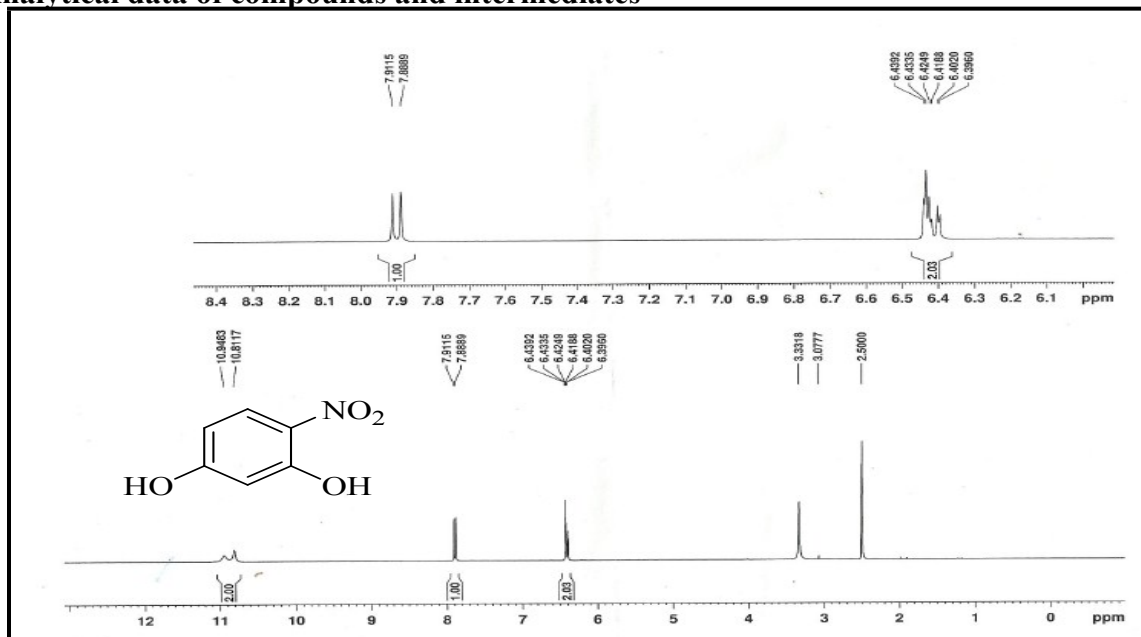


Fig. S1: ¹H NMR of compound 2 in DMSO-d₆.

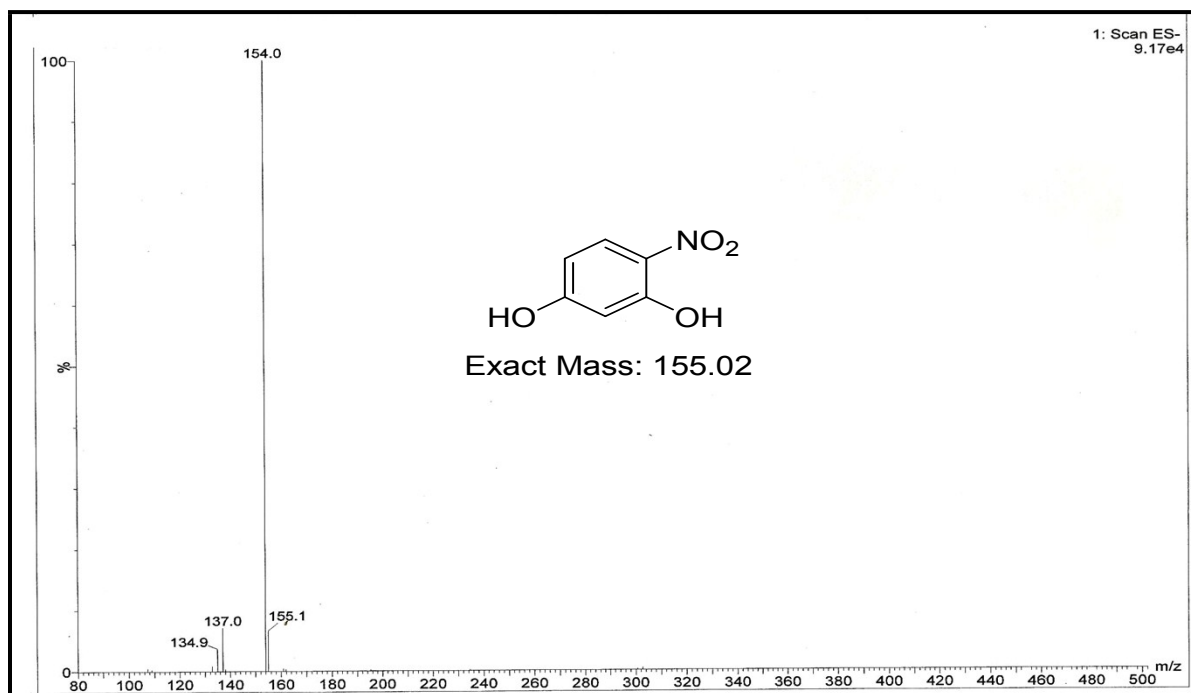


Fig. S2: ESI-MS of compound 2

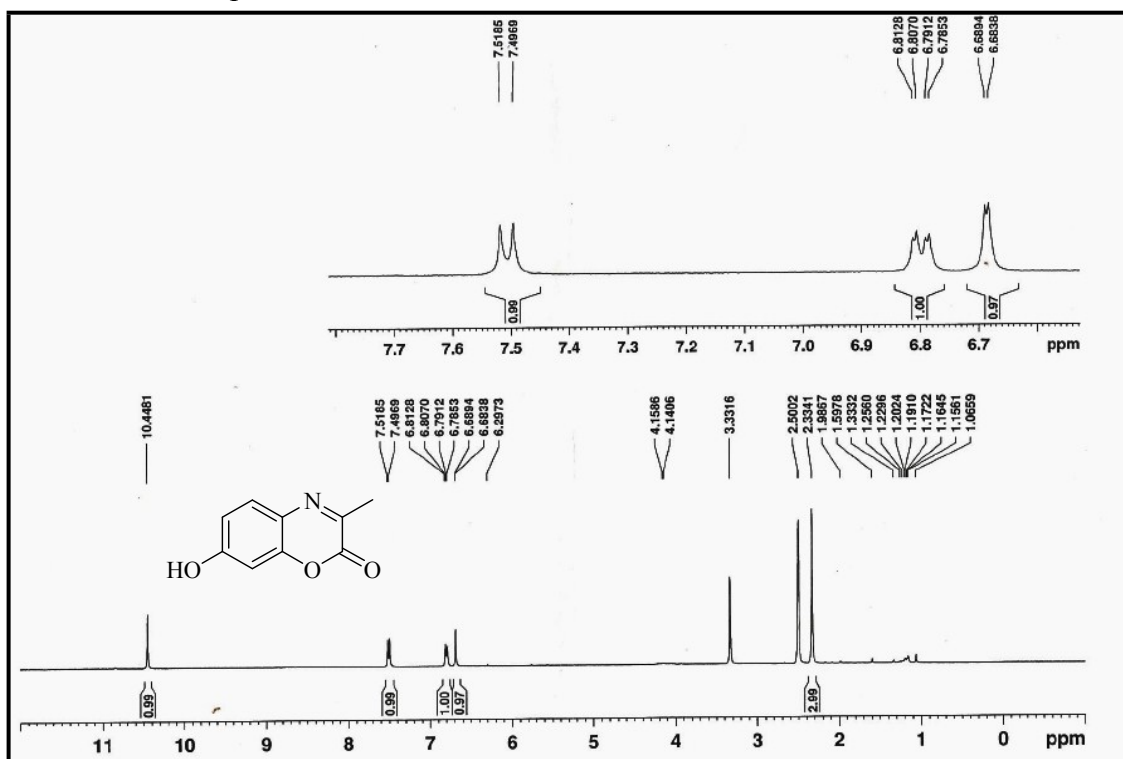


Fig. S3: ^1H NMR of compound **3** in DMSO- d_6

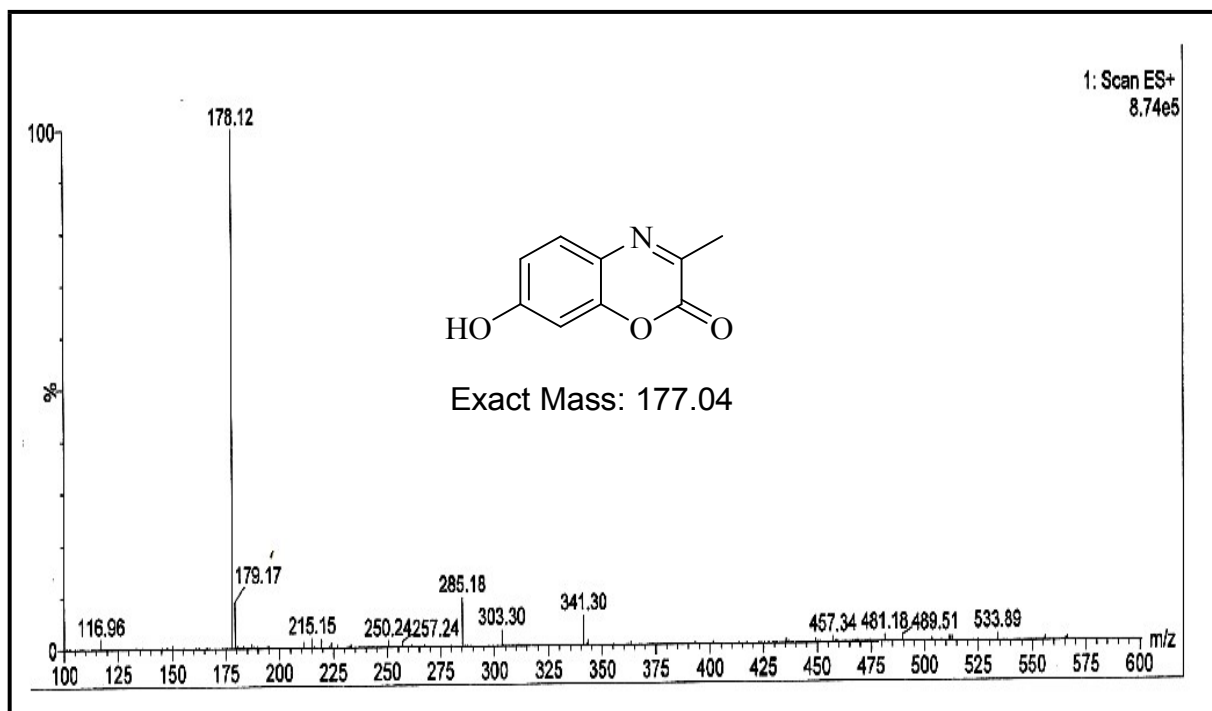


Fig. S4: ESI-MS of compound 3

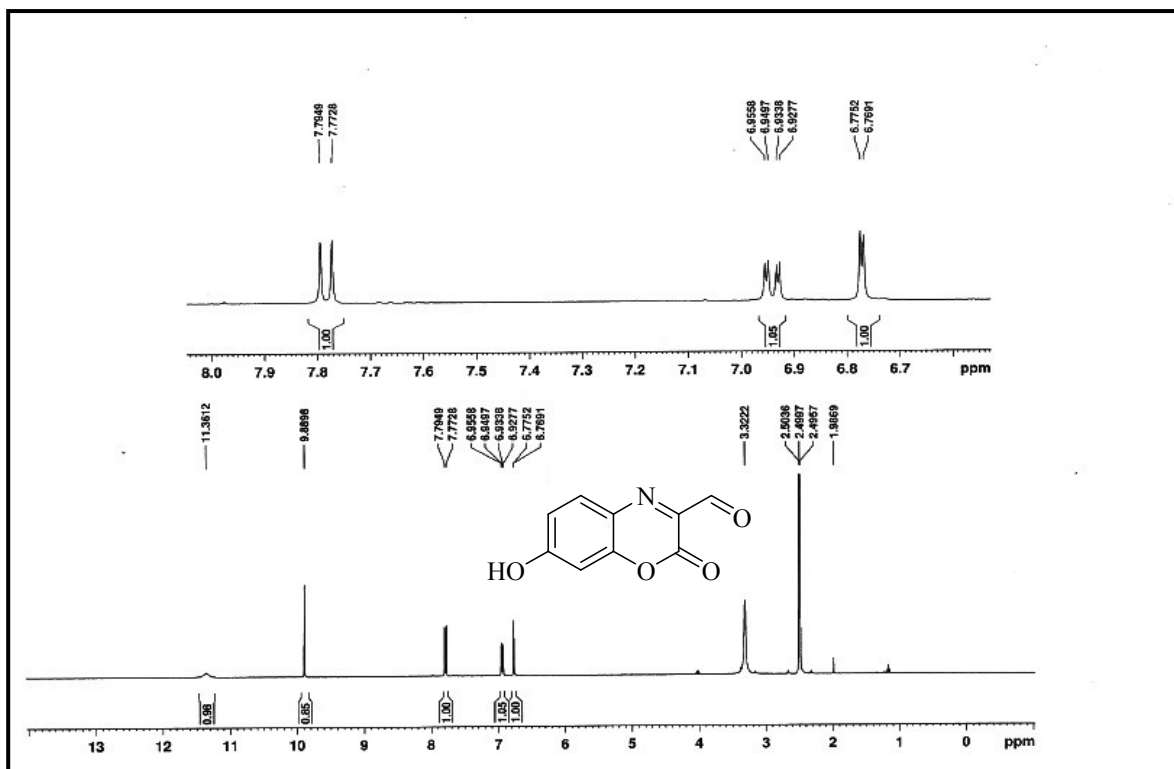


Fig. S5: ^1H NMR of compound **5** in DMSO-d_6

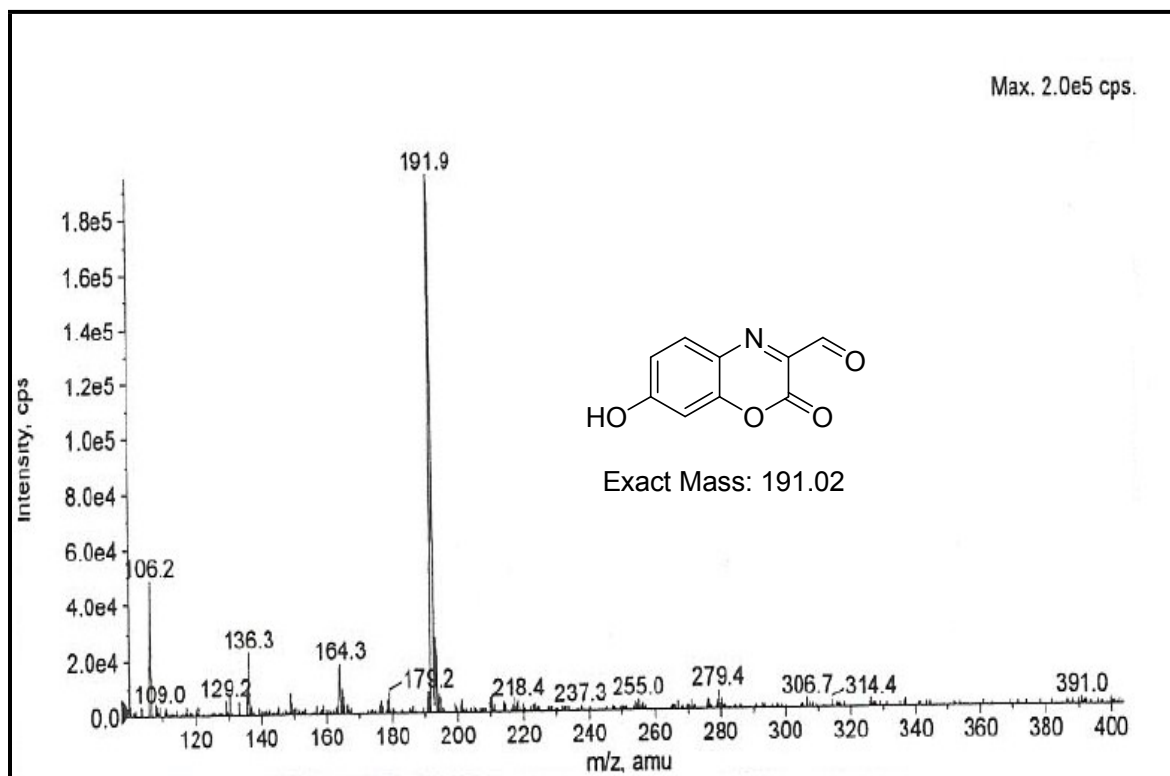


Fig. S6: ESI-MS of compound **5**

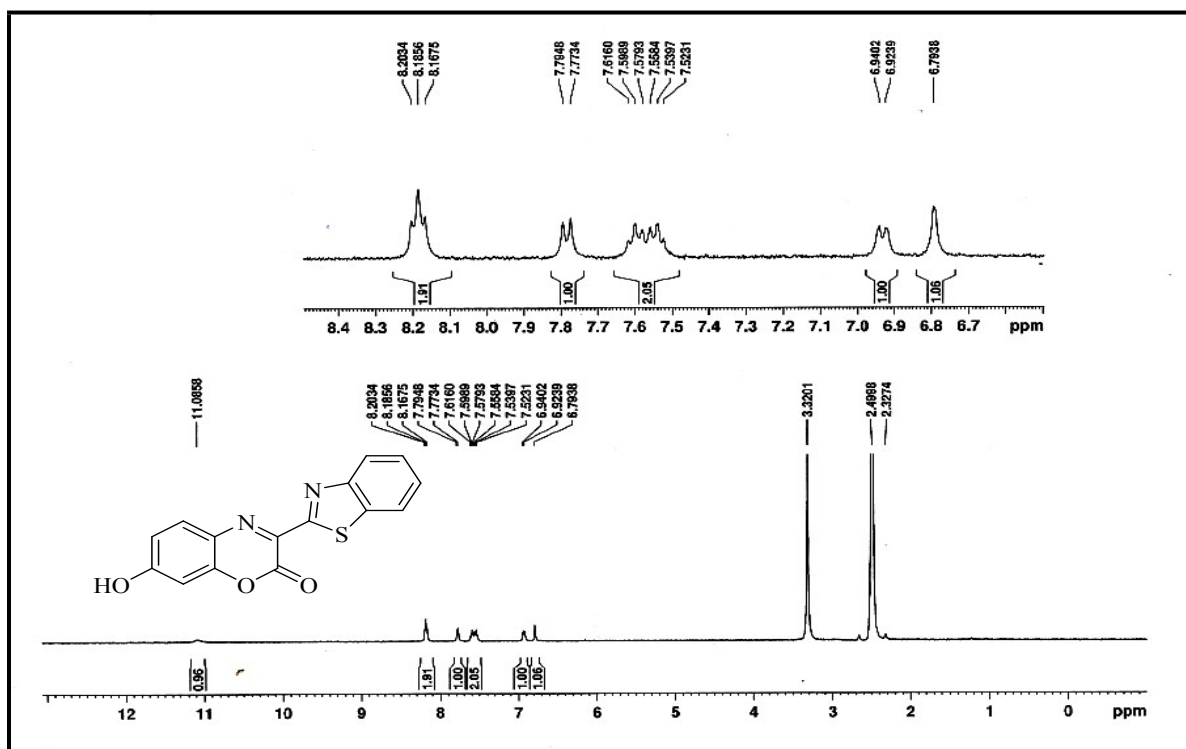


Fig. S7: ^1H NMR of compound **6** in DMSO-d_6

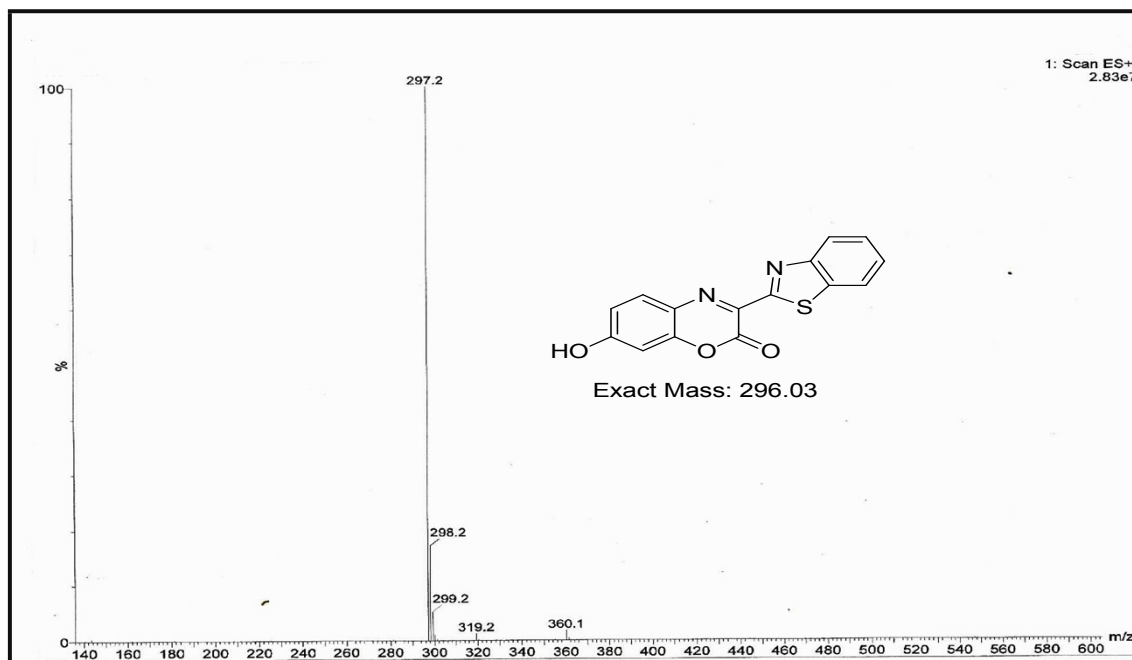


Fig. S8: ESI-MS of Compound **6**

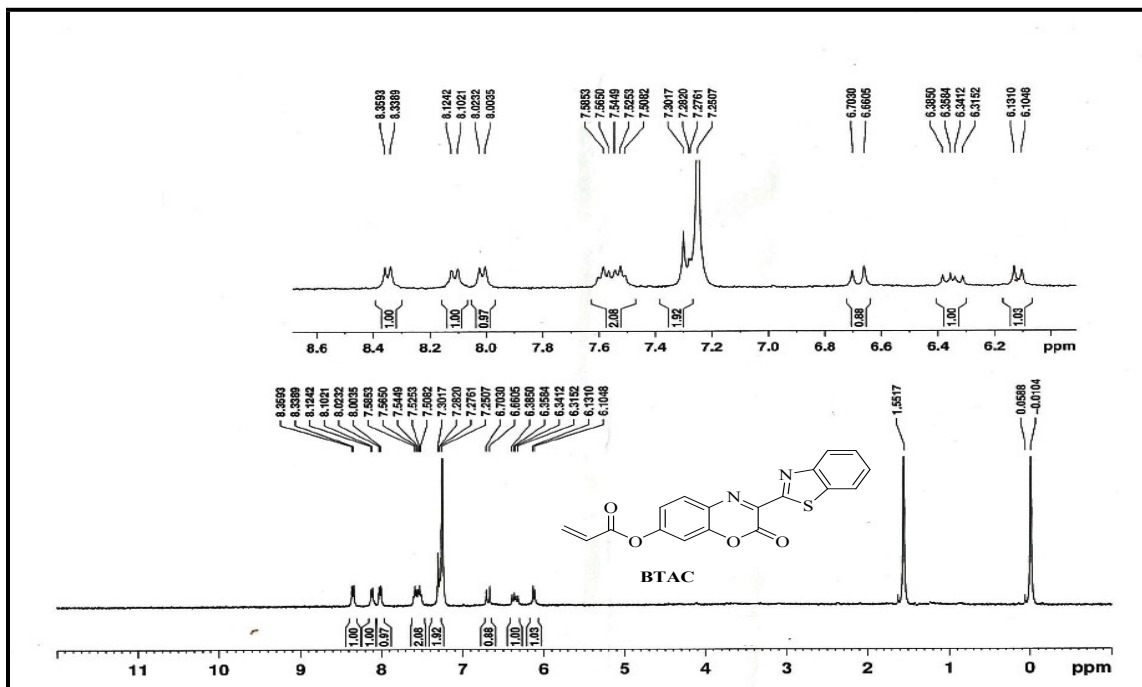


Fig. S9: ^1H NMR of Probe **BTAC** in CDCl_3

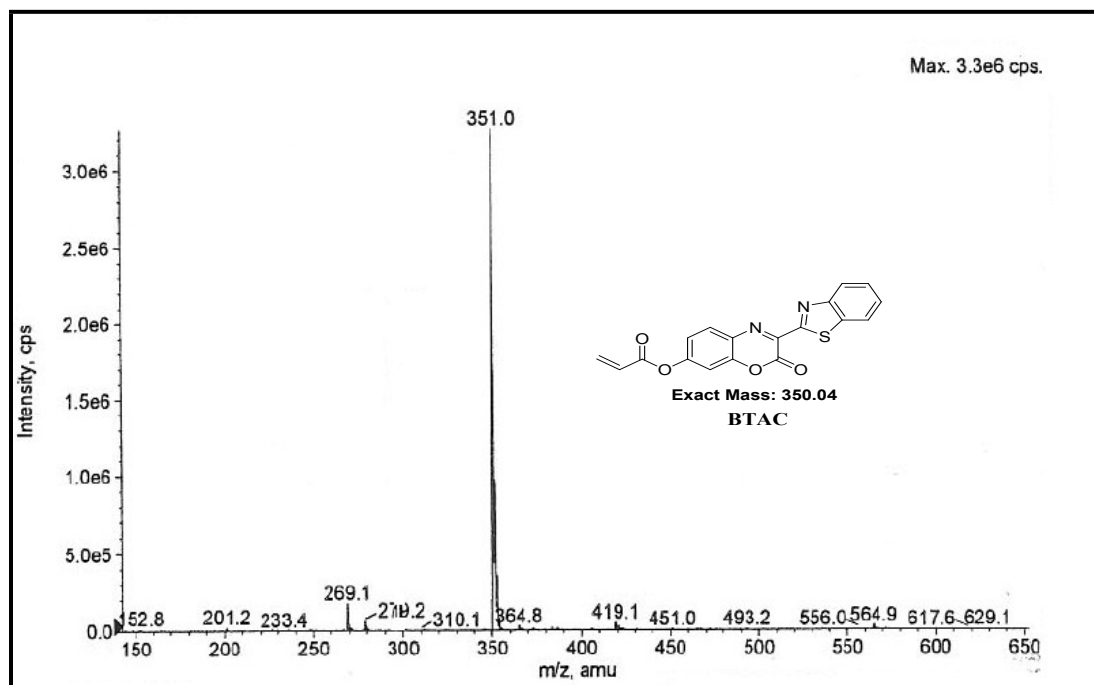


Fig. S10: ESI-MS of Probe **BTAC**

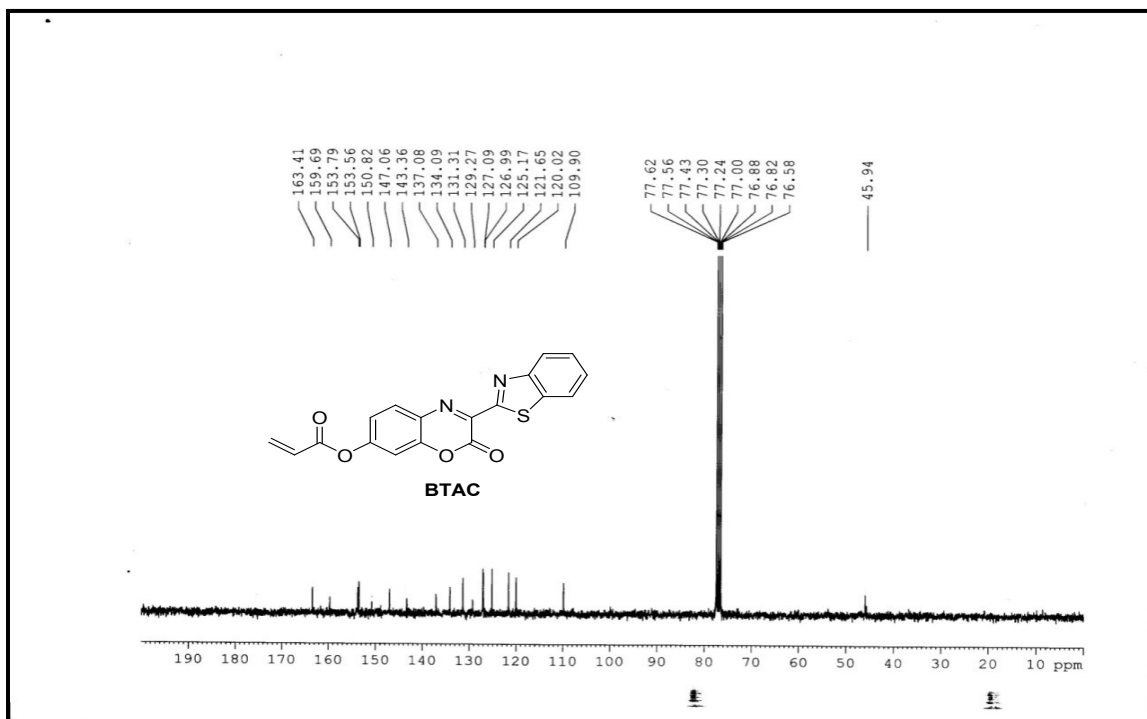


Fig. S11: ^{13}C NMR spectra of **BTAC** in DMSO-d_6

Calculations for detection limit

The detection limit (DL) of **BTAC** for Cys were determined from the following equation:

$$\text{DL} = K * \text{Sb1}/S$$

Where $K = 2$ or 3 (we take 2 in this case); Sb1 is the standard deviation of the blank solution; S is the slope of the calibration curve.

From graph $\text{Sb1}=0.49467$, $S=7.94964\text{E}8$. $\text{DL}= 1.24 \times 10^{-7}\text{M} = \mathbf{0.124 \mu\text{M}=124 \text{ nM}}$

$$\text{DL} = 2 \times 0.49467 / 7.94964\text{E}8 = 1.24 \times 10^{-7}\text{M} = 0.124 \mu\text{M} = 124 \text{ nM}$$

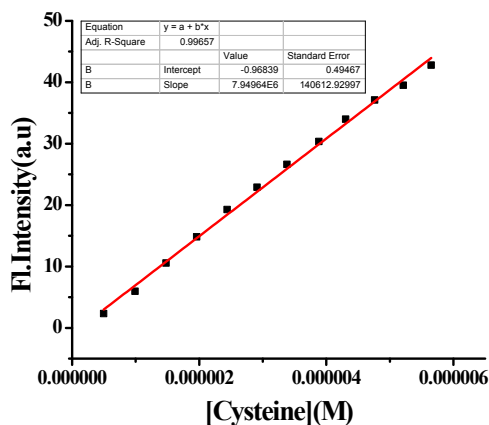


Fig. S12. Calibration curve for Fluorescence titration of BTAC at 560 nm with Cys.

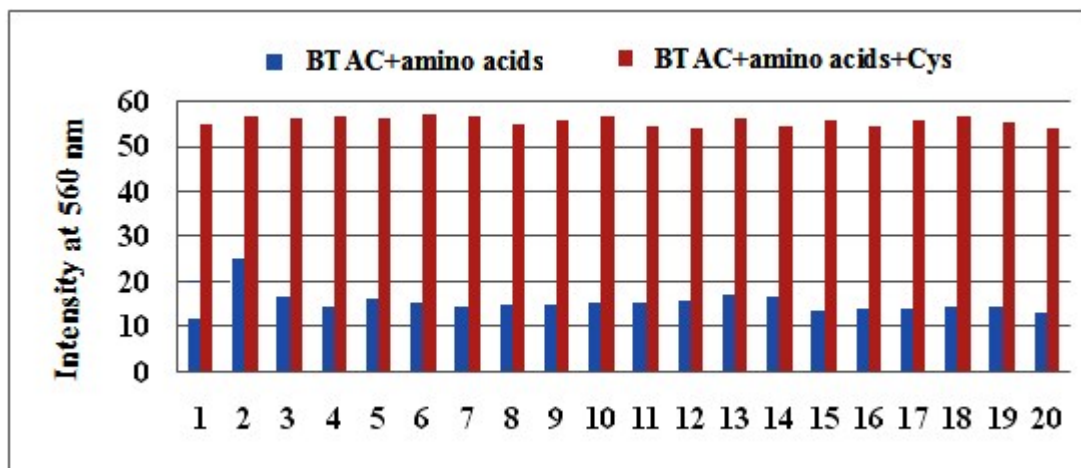


Fig. S13 (b) Fluorescence responses of BTAC (10 μ M) to Cys in the absence and presence of various amino acids (100 μ M) in aqueous DMSO (DMSO: H₂O = 4:1 v/v, 10 mM HEPES buffer, pH = 7.4). The blue bars represent the emission changes of BTAC in the presence of other amino acids (all were 100 μ M). The red bars represent the emission changes of BTAC with Cys in the presence of other amino acids. Various amino acids including: 1-Blank, 2- Hcy, 3- GSH, 4- Glu, 5- Asp, 6- Val, 7- Phe, 8- Tyr, 9- Ala, 10- Ser, 11- Leu, 12- Arg, 13- Pro, 14- Thr, 15- Gly, 16- Trp, 17- Ile, 18- Lys, 19-Met and 20- His. The intensities were recorded at 560 nm.

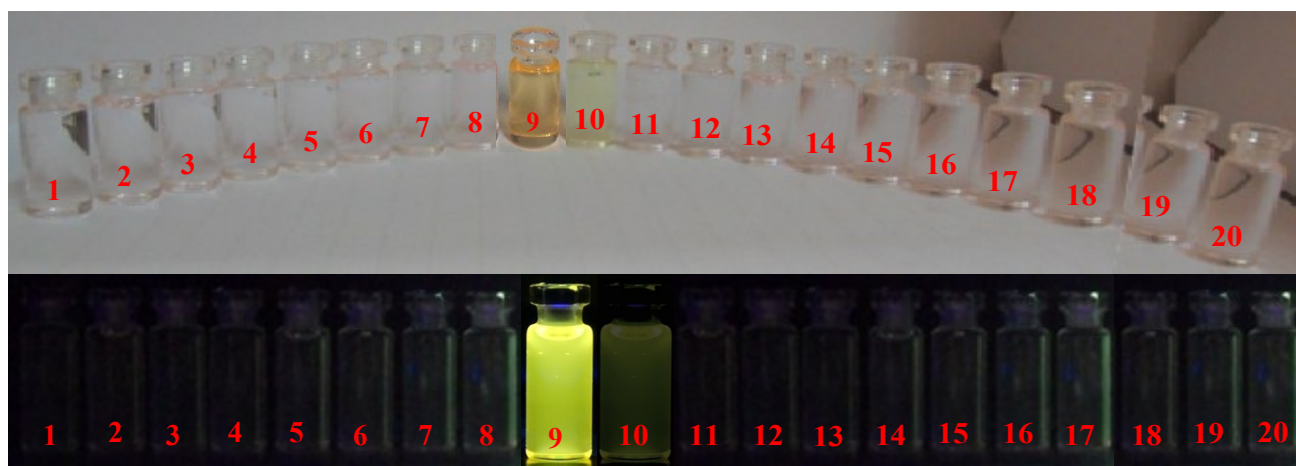


Fig. S14 : Visual color change (a) under daylight (b) handheld UV-lamp of probe BTAC (10 μ M) in presence of various amino acid (100 μ M) in aqueous DMSO (4:1 v/v, 10 mM HEPES buffer, pH = 7.4) at room temperature. (from left to right): 1- Glu, 2- Asp, 3- Val, 4- Phe, 5- Tyr, 6- Ala, 7- Ser, 8- Leu, 9-Cys, 10- Hcy, 11- GSH, 12- Arg, 13- Pro, 14- Thr, 15- Gly, 16- Trp, 17- Ile, 18- Lys, 19-Met and 20- His.

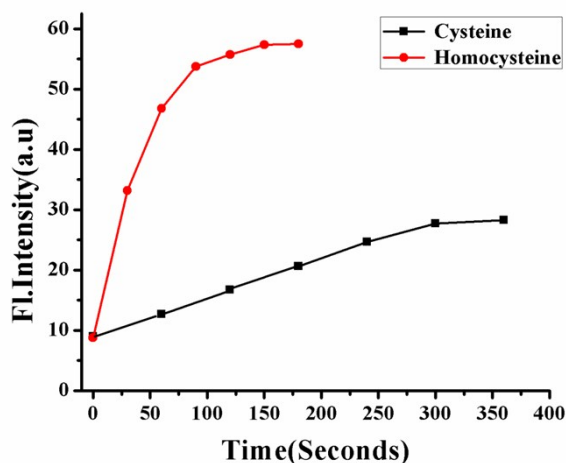


Fig. S15: Comparison of the time dependent fluorescence responses of BTAC (10 μM) in presence of Cys and Hcy in aqueous DMSO (DMSO: H_2O = 4:1 v/v, 10 mM HEPES buffer, pH = 7.4).

Kinetic Studies

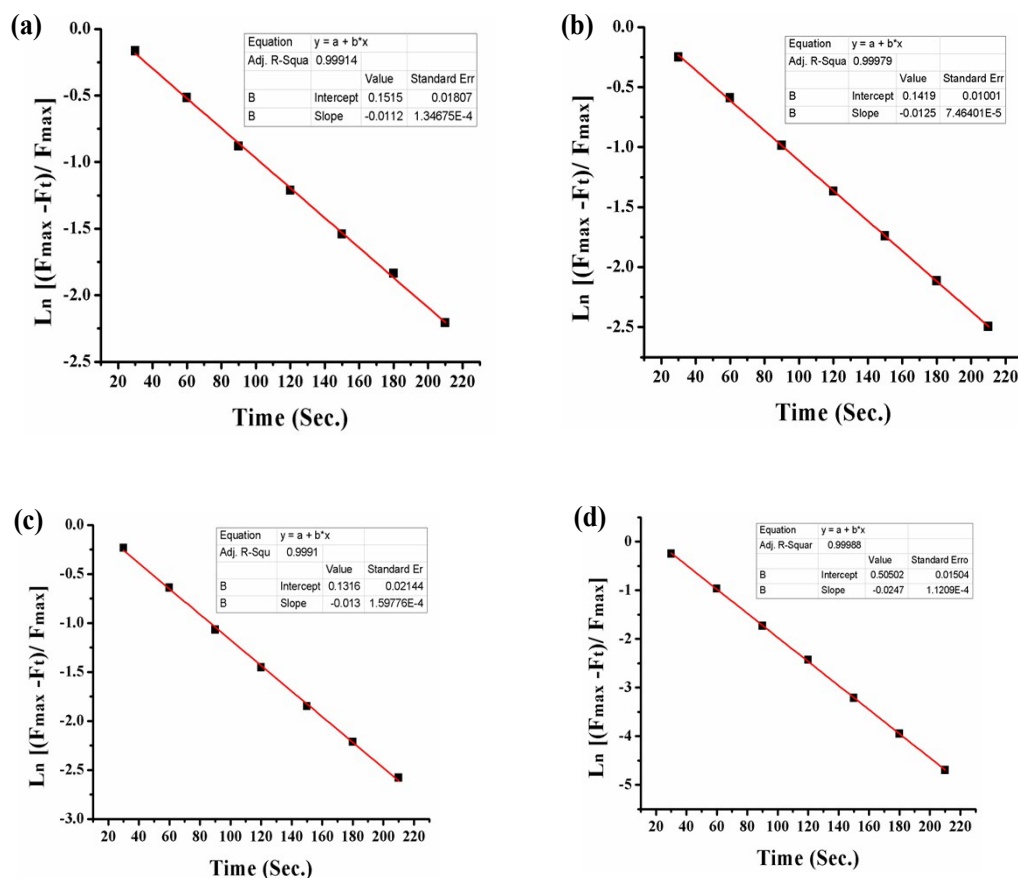


Fig. S16: (a) Pseudo first-order kinetic plot of reaction of BTAC (10 μM) with Cys (100 equiv.), slope = -0.0112 sec^{-1} . (b) Kinetic plot of BTAC with 25 equiv. Cys (c) Kinetic plot of BTAC with 50 equiv. Cys (d) Kinetic plot of BTAC with 80 equiv. Cys in (10 mM, pH 7.4, with 30% DMSO, 4:1, v/v).

The second-order rate constant for this reaction is thus the slope of a linear plot of k' versus the concentration of Cys (Fig.S17): $k = 2.674 \text{ M}^{-1}\text{Sec}^{-1}$

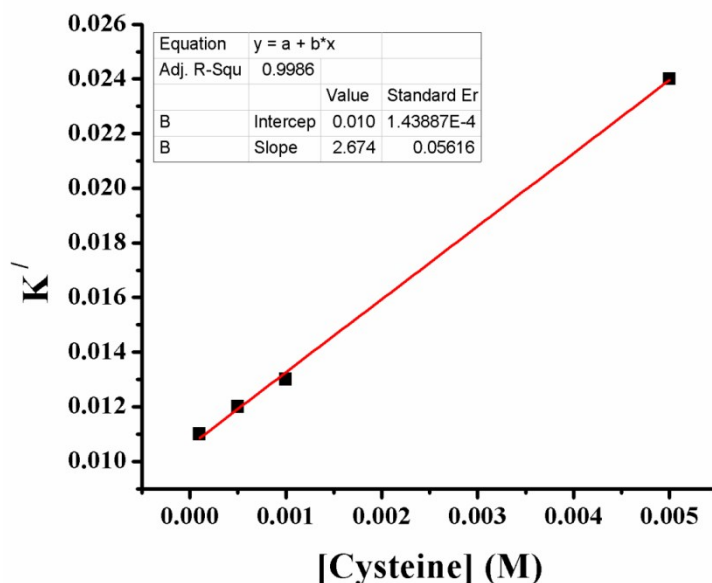


Fig. S17: Plot of the observed k' versus the concentration of Cys for the pseudo first-order reaction of BTAC (10 μ M) with varying concentration of Cys (10-150 Eq). **Slope = 2.674 M⁻¹Sec⁻¹.**

Cytotoxic effect on Cells

Human adult dermal fibroblast (HADF, Himedia Laboratories, India) cells were culture in Dulbecco's modified eagle medium (Gibco, NY) supplemented with 10% fetal bovine serum (FBS, Gibco, NY) and 1% antibiotic-antimycotic solution (Gibco, NY) and maintained at 37°C in a humidified CO₂ incubator. HADF cells were seeded in 24 well plates and allowed to growth for 24 h. Cells were treated with 10⁻⁵ M **BTAC** for 1h followed by treatment with 10⁻⁴ M **Cys** for 1 h. One well was set as negative control, well without treatment. Cells were washed with PBS and fluorescence microscopy was carried out under Nikon Inverted microscope (Nikon eclipse TiU, Japan) equipped with 20x (S Plan Fluor) objective. Excitation filters was used as 510-535 nm band pass filter and images were captured through 555-615 nm emission filter. The cytotoxic effects of the **BTAC** and **Cys** were determined by MTT as per manufacturer protocol (Himedia). Briefly, HADF cells (10³ cells/ well) were treated with 10⁻⁵ M **BTAC** in DMEM for

1 h followed by another 1 h with 10^{-4} M Cys. A blank (medium only) and a control (cell only) were set. After incubation, cells were washed with PBS and (3-(4,5-dimethylthiazol-2-yl)-2,5-diphenyltetrazolium bromide) (MTT) solution was added with DMEM medium. The plate was incubated for 4 h at 37°C. Solubilization solution was added to solubilize formazan.

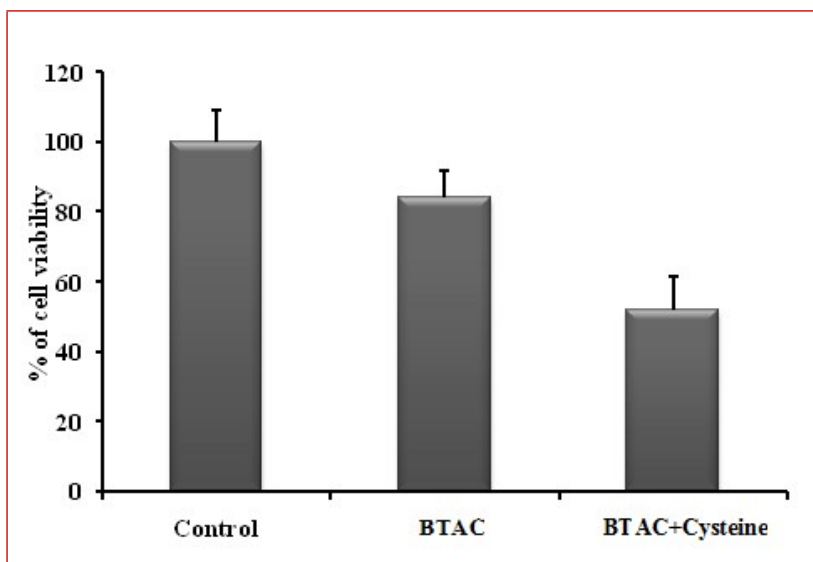


Fig. S18: Cell viability assay of HADF cells to observe the cytotoxic effect of **BTAC** and cysteine

Computational studies

Geometries have been optimized using the B3LYP/6-31G(d,p) level of theory in Gaussian 09. The geometries are verified as proper minima by frequency calculations. Time-dependent density functional theory calculation has also been performed at the same level of theory.

Table S1. Selected Electronic Excitation Energies (eV), Oscillator Strengths (f), Main Configurations, and CI Coefficients of the low-lying Excited States of BTAC and BTAC-O⁻. The data were calculated by TDDFT//B3LYP/6-31G(d,p) based on the optimized ground state geometries.

Molecules	Electronic Transition	Excitation Energy ^a	f ^b	Composition ^c
BTAC	S ₀ → S ₁	2.9694 eV 417.54 nm	0.1567	H-1 → L (58.2%)
	S ₀ → S ₂	3.0730 eV 403.47 nm	0.7892	H-1 → L (40.6%) H → L (58.4%)
BTAC-O⁻	S ₀ → S ₁	2.8665 eV 432.52 nm	0.9742	H → L (99.6%)

[a] Only selected excited states were considered. The numbers in parentheses are the excitation energy in wavelength. [b] Oscillator strength. [c] H stands for HOMO and L stands for LUMO.

Table S2. Energies of the highest occupied molecular orbital (HOMO) and lowest unoccupied molecular orbital (LUMO)

Species	E_{HOMO} (a.u)	E_{LUMO}(a.u)	ΔE(a.u)	ΔE(eV)	ΔE(kcal/mol)
BTAC	-0.22702	-0.10598	0.12104	3.293666	75.95
BTAC-O⁻	-0.06643	0.03645	0.10288	2.799529	60.6